

An Impeller Blade Analysis of Centrifugal Gas Compressor Using CFD

Vivek V. Kulkarni

*Department of Mechanical Engineering
KLS Gogte Institute of Technology, Belagavi, Karnataka*

Dr. Anil T.R.

*Department of Mechanical Engineering
KLS Gogte Institute of Technology, Belagavi, Karnataka*

Dr. Rajan N.K.S.

*Department of Aerospace Engineering
Indian Institute of Science, Bangalore, Karnataka*

Abstract- Compressor characteristics, being representations of the compressor pressure ratio as a function of producer gas flow through the compressor, have been studied. Centrifugal compressors are used in turbochargers to increase the pressure of air and also its density greater than ambient. Choosing the right compressor is very important in obtaining best power output of engine by turbocharging, so it is important to have compressor map for matching turbocharger with a particular engine. Compressor map is drawn by running turbocharger's compressor at varying speeds and mass flow rates. The compressor map along with other operating variables is generated for varying speeds and on the compressor map surge line and choke line are drawn. In this research work, the centrifugal compressor characteristics were investigated through CFD analysis using industry standard software ANSYS-V13.

Keywords – Producer gas, Centrifugal compressor, Pressure ratio, Mass flow rate, Computational Fluid Dynamics

I. INTRODUCTION

Besides the pressurization and transportation of fluids in the process and chemical industries, other applications of centrifugal compressors involve fluid compression for use in aircraft engines, in industrial gas turbines and in turbocharged combustion engines [1]. Centrifugal compressors have an instable working region. In this region, a decrease of flow results in a decrease of outlet pressure. When the plenum pressure behind the compressor is higher than the compressor outlet pressure, the fluid tends to reverse or even flow back in the compressor. As a consequence, the plenum pressure will decrease, inlet pressure will increase and the flow reverses again. This phenomenon, called surge, repeats and occurs in cycles with frequencies varying from 1 to 2 Hz [2]. Another aerodynamic instability that can occur in centrifugal compressors is stall. Both instabilities dramatically decrease the efficiency and severe surge can even cause mechanical damage to the compressor.

The working principle of a centrifugal compressor is to increase the kinetic energy of the fluid with a rotating impeller. The fluid is then slowed down in a volume called the plenum, where the kinetic energy is converted into potential energy in the form of a pressure rise. Hence compression is achieved by transferring momentum to the fluid and the subsequent diffusion to convert the kinetic energy into pressure. The momentum transfer takes place at the curved blades of the impeller that is mounted on a rotating shaft. Diffusion takes place in the annular channel of increasing radius around the impeller, usually referred to as diffuser [3].

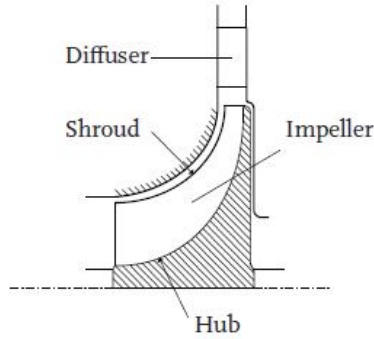


Figure 1. Impeller blade of centrifugal compressor [3]

Figure 1 shows the sketch of a rotating *impeller* that imparts a high velocity to the fluid, and a number of fixed diverging passages in which the fluid is decelerated with a consequent rise in static pressure in the plenum. The latter process is one of diffusion, and thus the part of the compressor containing the diverging passages is known as the *diffuser*. Fluid enters the impeller eye and is whirled around at high rotational speed (by the vanes or without the vanes) on the impeller disc. The static pressure rise is obtained in the diffuser, where very high velocity of the fluid, leaving the impeller tip, is reduced to a velocity similar to the velocity of the fluid entering the impeller eye [2]. The performance of a compressor can be graphically depicted in a so-called compressor map. An example is shown in Figure 2. The *surge line* connects points from whereon surge can occur. Surge is associated with a drop in delivery pressure, and with violent aerodynamic pulsations that are transmitted throughout the whole machine.

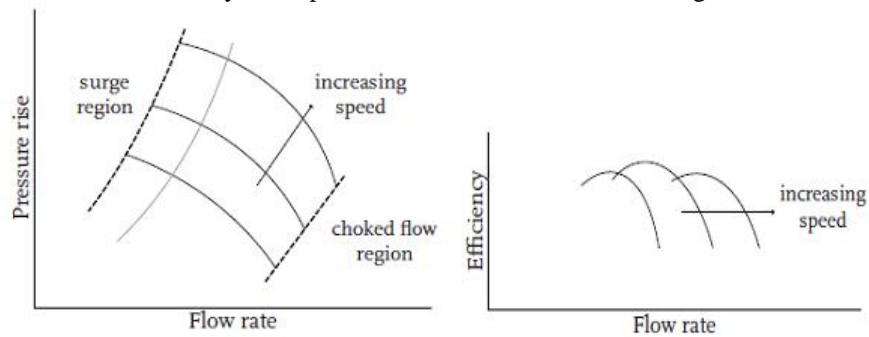


Figure 2. Characteristic maps of a centrifugal compressor [2].

As visualized in Figure 2, the part left of the surge line has positive slope and this is the region where surge can occur. A safety margin is taken into account, resulting in a new line called the *surge avoidance line*. The task of the surge avoidance controller is to prevent the compressor from operating in a point in the compressor map that is located to the left of the surge avoidance line [2]. The individual characteristic curves or speed lines are formed by steady-state operating points with the same rotational speed. The achievable flow rates are limited by the occurrence of surge at low flows and the phenomenon known as choking at high flows. Choking occurs when the local velocity, usually in the impeller exit or diffuser, reaches the speed of sound.

II. PROPOSED METHODOLOGY

A. Modelling of an Impeller –

The impeller considered in the present study consists of 8 main blades and 8 splitter blades. The tip clearance between the blade tip and shroud surface is 0.1mm. The impeller geometry was designed using BladeGen workbench in ANSYS 13V. The details of impeller geometry are shown in Table 1.

Table -1 Details of impeller geometry

| Blade information | Backward swept |
|-------------------------------|----------------|
| No. of blades (main+splitter) | 8+8 |
| Eye radius, r_e | 8.8 mm |

| | |
|--------------------------------------|--------------|
| Eye tip radius, r_t | 24.42 mm |
| Impeller exit radius, r_i | 36.4 mm |
| Blade height at impeller exit, h_e | 4.67 mm |
| Hub beta at LE, β_{h1} | 14.7° |
| Tip beta at LE, β_{t1} | 50.5° |
| Hub beta at TE, β_{h2} | 19.1° |
| Tip beta at TE, β_{t2} | 17.1° |

Figure 3 shows the three dimensional view of impeller obtained by details mentioned in Table1 and the larger blade is the main blade and the smaller blade is splitter blade. To reduce the computation time, one passage of the blade consisting of one main blade and one splitter blade is meshed and solved by applying periodic boundary conditions at each side of blade passage.

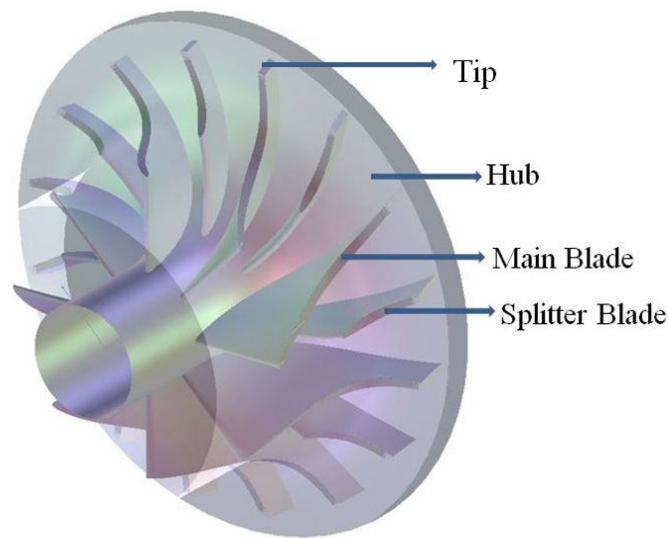


Figure 3. 3D view of an impeller

B. Grid generation –

The grid is generated using TurboGrid workbench approach in ANSYS 13. It consists of hexahedral cells of HJCL-type of grid with O-grid around the blades. There are 493521 nodes in a passage which includes one main blade and one splitter blade with periodic boundary conditions. Fig. 4 shows grid generated to one passage of impeller.

The boundary conditions applied are total pressure and total temperature at inlet and mass flow at outlet and the impeller rotation speeds were also specified. The CFD solver used is CFX which is commercially available CFD software and the boundary conditions used are P-total and T-Total at inlet and mass flow rate at outlet. The standard Shear Stress Transport (SST) $k-\omega$ turbulence model is used for. The residual target set for the simulation is $1e^{-6}$ and at lower mass flow rates the convergence achieved was between $1e^{-3}$ and $1e^{-6}$.

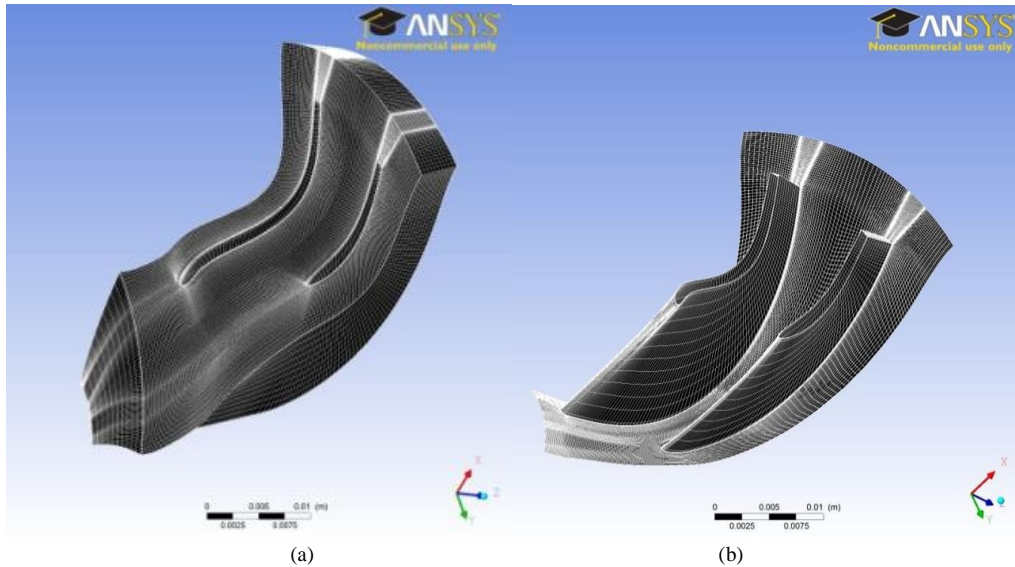


Figure 4. Mesh generated on impeller passage (a) and over blades (b)

The simulations with these boundary conditions are obtained for varying speeds and different parameters like impeller isentropic efficiency, total pressure ratio (P_r) are plotted at different mass flow rates. CFD contour plots and vector plots are also used to understand flow through the impeller and identify the regions of losses. The convergence criteria set for residuals is $1e^{-6}$. However at off design points where flow separation takes place and flow reversal occurs at the blades and the convergence achieved was between $1e^{-3}$ and $1e^{-6}$. All the walls are set as smooth walls with no slip wall condition. Figure 5 shows the blade profile after applying the said boundary conditions

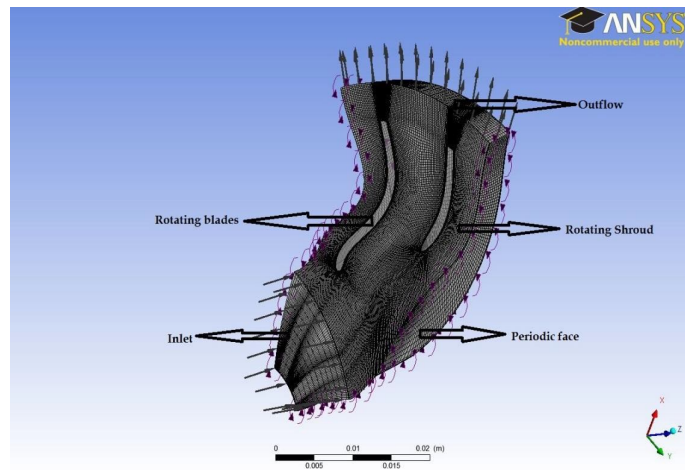


Figure 5. Boundary conditions applied for impeller

III. SIMULATION RESULTS AND DISCUSSIONS

A. Plot results of flow through an Impeller –

The various plots were plotted in CFX-post to understand the flow and performance characteristics of the compressor. In this paper, the discussion is carried out on the plots obtained for impeller for various speeds and mass flow rates. The flow through compressor impeller was solved for different speed starting from 40000 rpm to 50000 rpm with total pressure at inlet and mass flow boundary at outlet. The Figure 6 shows the contours of total pressure and velocity across the impeller blade in blade to blade view for $\dot{m} = 0.11$ kg/s and $N = 60000$ rpm. It can be seen from the plot that the pressure increases from leading edge to trailing edge and a low pressure region exists at just downstream of the of the leading edge which is due to flow separation at lower mass flow rates for given speed which results in stalling.

This signifies the increase in total pressure due to increase in velocity of the air which in turn due to energy transfers from rotating blade to flowing air from leading edge to trailing edge. In diffuser by converting this part of kinetic energy into pressure energy the total pressure can be increased substantially.

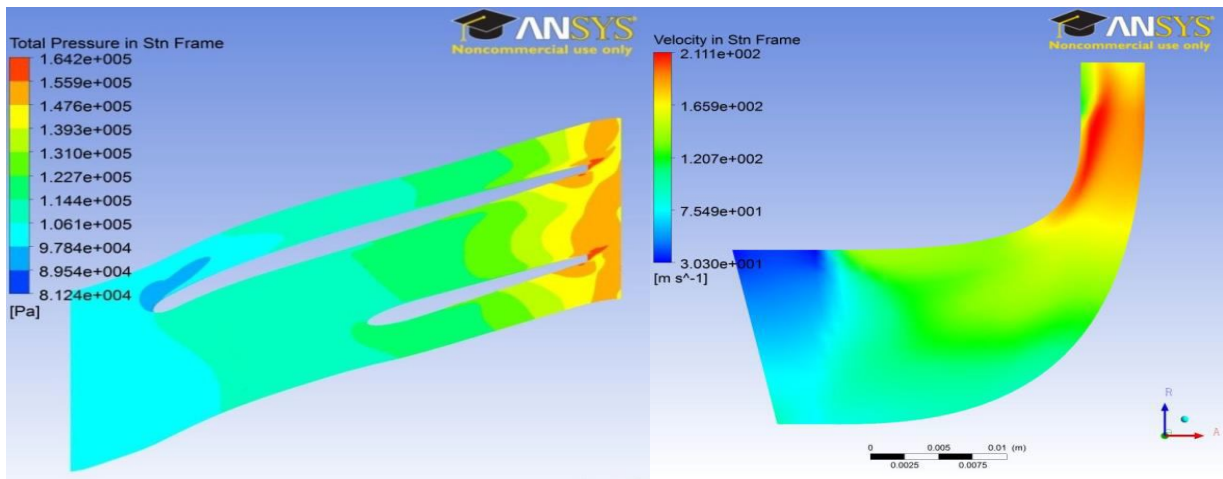


Figure 6. Contours of total pressure (a) and velocity (b) for $\dot{m} = 0.11$ kg/s and $N = 60000$ rpm at 0.5 span

When a gas is compressed its density and also the temperature increases as shown in Figure 7. Normally, in centrifugal compressors, as the mass flow rate is reduced below a critical value for any given rotational speed, the flow separation from blade takes place and results in stalling which later leads to surge or compressor instability.

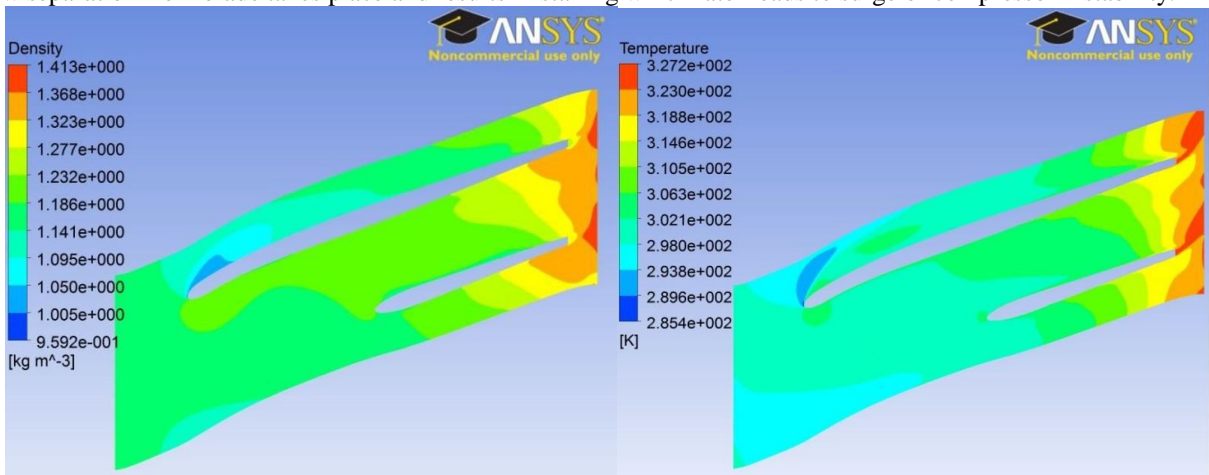


Figure 7: Contours of density (a) and temperature variation (b) for $\dot{m} = 0.11$ kg/s and $N = 60000$ rpm at 0.5 span

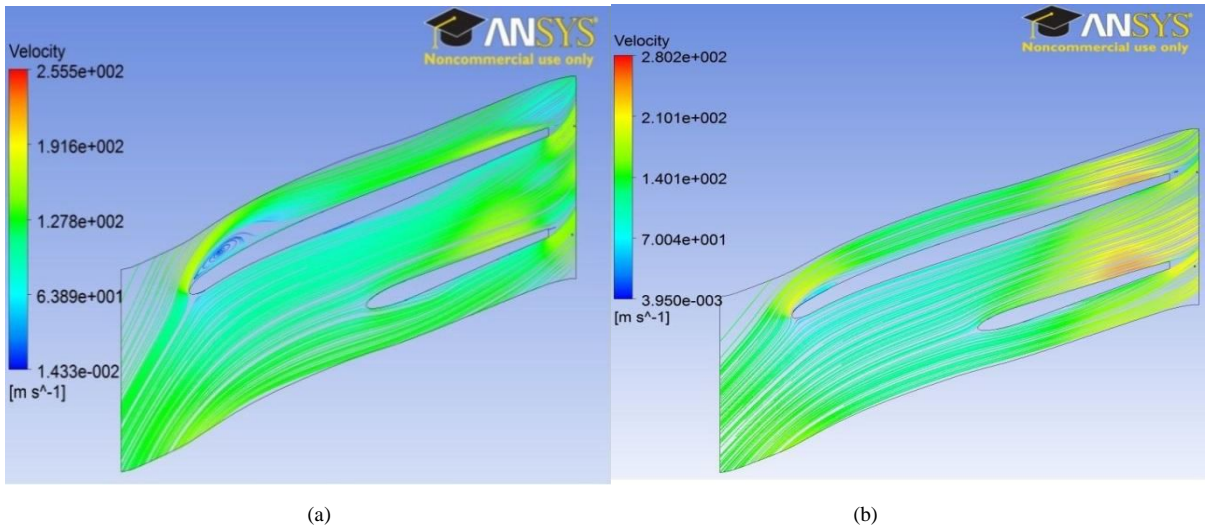


Fig. 8: Velocity streamlines for $\dot{m} = 0.11$ kg/s (a) and $\dot{m} = 0.16$ kg/s (b) at $N = 60000$ rpm and 0.5 span

Figure 8(a) and 8(b) shows the streamlines for $\dot{m} = 0.11$ kg/s and $\dot{m} = 0.16$ kg/s respectively. It can be observed that for $\dot{m} = 0.11$ kg/s, the flow separation occurs after the leading edge and it does not exist for $\dot{m} = 0.16$ kg/s. This flow separation is shown in 3D view in Figure. 9(a) and 9(b) shows tip leakage losses, which occurs due to pressure difference between forward face (pressure surface) and rear face (suction surface). This results in specific work reduction for any compressor and hence the tip clearance must be kept as low as possible and is limited by manufacturing constraints.

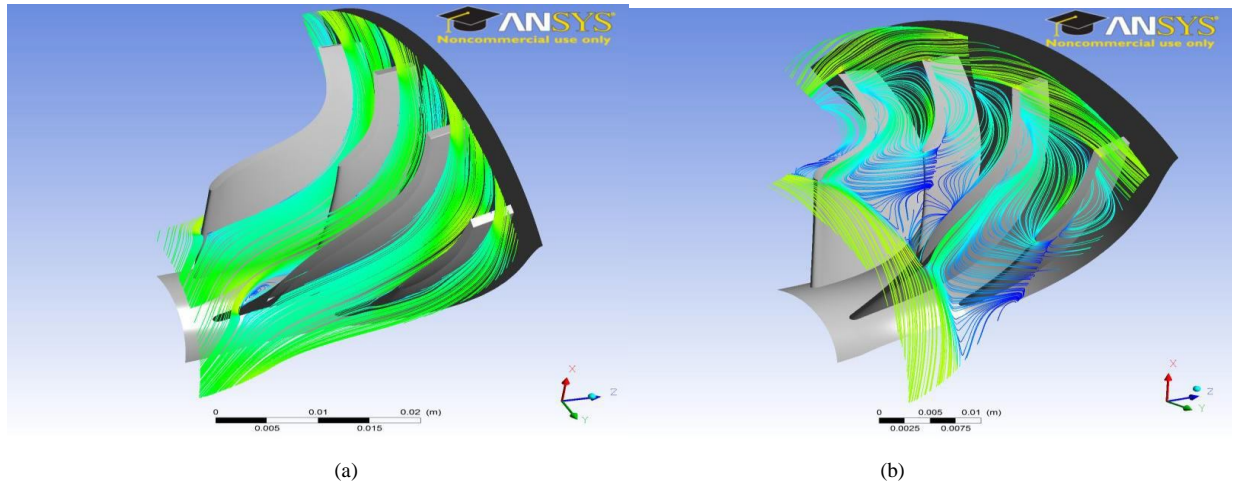


Figure 9: Flow separation near leading edge (a) and tip leakage (b) in 3D view for $\dot{m} = 0.11$ kg/s and $N = 60000$ rpm.

B. Characteristic Curves of Compressor –

The graphs were plotted with different mass flow rates vs. pressure ratios and different mass flow rates vs. isentropic efficiencies developed by compressor at different speeds and are shown in Fig. 10(a) and 10(b) respectively. From Fig. 11(a), it can be observed that the mass flow rate that the impeller can handle increases with the increase in its rotational speed i.e. at 40000 rpm the maximum value of mass flow rate that the impeller can handle is around 0.17 kg/s beyond which the sonic condition is reached and flow chokes and as this rotational speed increases to 80000, the maximum mass flow rate is around 0.19 to 0.2 kg/s and flow chokes beyond this point.

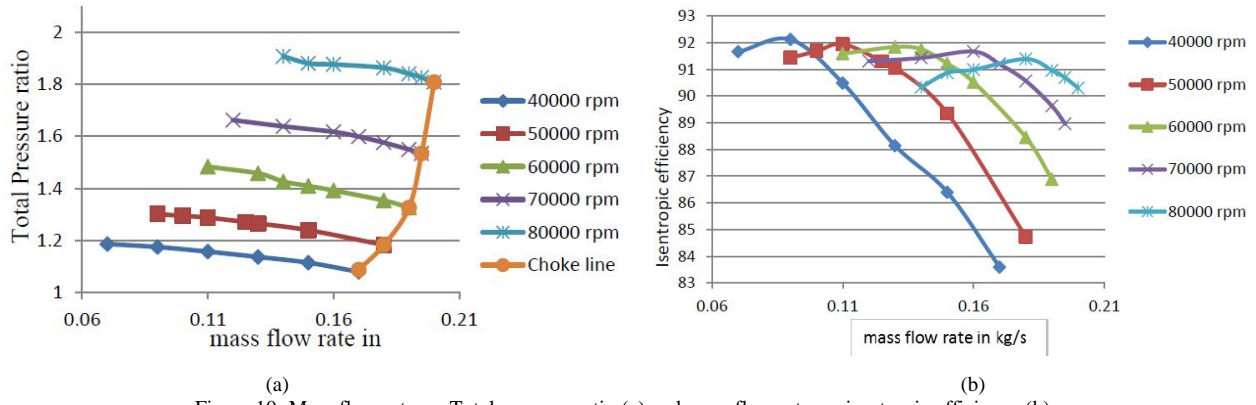


Figure 10: Mass flow rate vs. Total pressure ratio (a) and mass flow rate vs. isentropic efficiency (b).

Fig. 11(b) shows the graph of mass flow rate vs. isentropic efficiency for impeller. It can be observed that at all speeds, there is one maximum efficiency point and the efficiency increases with the increase in mass flow initially and at one point it reaches maximum value and start decreasing with further increase in mass flow. This is because, at peak efficiency point, the gas incidence angle matches with blade angles and with the decrease in mass flow rate gas incidence angles changes and results in flow separation from blade.

While, increase in mass flow rate after the peak efficiency point results in increase in absolute velocity of gas and when it reaches sonic speed, the flow chokes.

IV. CONCLUSION

The CFD simulations were carried out to understanding the flow characteristics through the impeller. Following are the conclusions drawn:

- It was observed that, during a flow through impeller, maximum mass flow rate that the impeller could handle was found to be around 0.2 kg/s and beyond this, sonic condition was reached as Mach number reached 1.
- As study is restricted to the performance of an impeller only, the compressor could handle relatively smaller mass flow rates, as there is not enough and effective diffusion taking place at the downstream of the impeller and the sonic conditions were reached early. This can be overcome by attaching a volute to the impeller.
- It can be observed from the streamline plots and contour plots that due to swirling flow, there are some pressure losses due to fluid friction.
- The kinetic energy available in air at the outlet of impeller was converted into pressure energy and it can be observed from graphs that the total pressure ratio is increasing as speed of the impeller increases.
- As the compressor characteristics are plotted at different conditions such as different mass flow rates and speeds, the data can be used for turbocharger analysis and engine matching.

REFERENCE

- [1] Saravanamuttoo, H.I.H., Rogers, G.F.C., Cohen, H. 'Gas Turbine Theory.' 2001.
- [2] Peter Tijl, Modeling, simulation and evaluation of a centrifugal compressor with surge avoidance control. DCT 2004.039, Traineeship report.
- [3] Jan van Helvoir, Centrifugal Compressor Surge, Modeling and Identification for Control, Technical Universities Eindhoven, 2007.